Radiology

Contrast-enhanced MR Imaging versus Contrast-enhanced US: A Comparison in Glioblastoma Surgery by Using Intraoperative Fusion Imaging[1]

Francesco Prada, MD
Valerio Vitale, MD
Massimiliano Del Bene, MD
Carlo Boffano, MD
Luca Maria Sconfienza, MD, PhD
Valentina Pinzi, MD
Giovanni Mauri, MD
Luigi Solbiati, MD
Georgios Sakas, MD
Velizar Kolev, MD
Ludovico D'Incerti, MD
Francesco DiMeco, MD

Purpose: To compare contrast material enhancement of glioblastoma multiforme (GBM) with intraoperative contrast-enhanced ultrasonography (US) versus that with preoperative gadolinium-enhanced T1-weighted magnetic resonance (MR) imaging by using real-time fusion imaging.

Materials and Methods: Ten patients with GBM were retrospectively identified by using routinely collected, anonymized data. Navigated contrast-enhanced US was performed after intravenous administration of contrast material before tumor resection. All patients underwent tumor excision with navigated intraoperative US guidance with use of fusion imaging between real-time intraoperative US and preoperative MR imaging. With use of fusion imaging, glioblastoma contrast enhancement at contrast-enhanced US (regarding location, morphologic features, margins, dimensions, and pattern) was compared with that at gadolinium-enhanced T1-weighted MR imaging.

Results: Fusion imaging for virtual navigation enabled matching of real-time contrast-enhanced US scans to corresponding coplanar preoperative gadolinium-enhanced T1-weighted MR images in all cases, with a positional discrepancy of less than 2 mm. Contrast enhancement of gadolinium-enhanced T1-weighted MR imaging and contrast-enhanced US was superimposable in all cases with regard to location, margins, dimensions, and morphologic features. The qualitative analysis of contrast enhancement pattern demonstrated a similar distribution in contrast-enhanced US and gadolinium-enhanced T1-weighted MR imaging in nine patients: Seven lesions showed peripheral inhomogeneous ring enhancement, and two lesions showed a prevalent nodular pattern. In one patient, the contrast enhancement pattern differed between the two modalities: Contrast-enhanced US showed enhancement of the entire bulk of the tumor, whereas gadolinium-enhanced T1-weighted MR imaging demonstrated peripheral contrast enhancement.

Conclusion: Glioblastoma contrast enhancement with contrast-enhanced US is superimposable on that provided with preoperative gadolinium-enhanced T1-weighted MR imaging regarding location, margins, morphologic features, and dimensions, with a similar enhancement pattern in most cases. Thus, contrast-enhanced US is of potential use in the surgical management of GBM.

Online supplemental material is available for this article.

[1] From the Department of Neurosurgery (F.P., M.D.B., F.D.), Department of Neuroradiology (C.B., L.D.), and Radiotherapy Unit (V.P.), Fondazione IRCCS Istituto Neurologico "C. Besta," Via Celoria n.11, 20133 Milan, Italy; Department of Imaging and Radiation Therapy, Azienda Socio-sanitaria Territoriale di Lecco, Lecco, Italy (V.V.); Radiology Unit, IRCCS Policlinico San Donato, San Donato Milanese, Italy (L.M.S.); Department of Biomedical Sciences for Health, University of Milan, Milan, Italy (L.M.S.); Department of Interventional Radiology, Istituto Europeo di Oncologia, Milan, Italy (G.M.); Department of Radiology, Humanitas Research Hospital, Rozzano, Italy (L.S.); Department of Research and Development, MedCom, Darmstadt, Germany (G.S., V.K.); and Department of Neurologic Surgery, Johns Hopkins Medical School, Baltimore, Md (F.D.). From the 2016 RSNA Annual Meeting. Received May 25, 2016; revision requested July 25 and received October 31; accepted December 16; final version accepted February 26, 2017. **Address correspondence to** F.P. (e-mail: *francesco.prada@istituto-besta.it*).

Supported by the Seventh Framework Programme (grant 602 923).

Glioblastoma multiforme (GBM) is the most aggressive and frequent subtype of astrocytoma, representing 15.6% of all primary nervous system tumors (1). The treatment protocol is based on surgical resection followed by radiation therapy and chemotherapy (2). Surgery, in particular the extent of resection, has a direct influence on the prognosis of patients with GBM. Thus, the actual goal of surgery is to resect the entire enhancing tumor seen at preoperative gadolinium-enhanced T1-weighted magnetic resonance (MR) imaging (3–5). In this effort, intraoperative imaging is pivotal and the alternatives various: neuronavigation, fluorescence-enhanced imaging, and proper intraoperative imaging (MR imaging, computed tomography [CT], and ultrasonography [US]).

Intraoperative neuronavigation is based on preoperative gadolinium-enhanced T1-weighted MR imaging and is accurate in planning the craniotomy and during the initial stages of surgery. On the other hand, after bone removal, as surgery progresses, brain shift and brain deformation take place, making the information from neuronavigation unreliable (6–8).

Fluorescence-guided surgery represents a different approach. It is based on direct fluorescent dyes (fluorescein) or dyes that must be metabolized by tumor cells (5-aminolevulinic acid) (9). In both cases, the principal drawback is the need to expose the surface of the tumor in order to evaluate the location of the dye; thus, this technique is limited in assessments of the deep margins of the tumor.

Another solution is the use of intraoperative MR imaging, CT, or US (10–14). The first two modalities take into account brain shift and modifications and allow updating of the neuronavigation system (10,11). The major limitations of these imaging techniques are the limited availability, high costs, and prolongation of total operative time.

A more practical and cost-efficient tool for planning and guiding surgeries is intraoperative US (7,12–15). It enables acquisition of real-time information during and after tumor resection but suffers from several artifacts and lack of training by most neurosurgeons. However, when coupled with navigation systems, orientation is improved and the brain shift can be compensated for, with improved orientation and image interpretation (7,12–16). Some investigators have shown that US applied to neuronavigation systems improves patient survival in the resection of GBM (13,17). With fusion imaging for virtual navigation, preoperative MR images and real-time intraoperative US scans can be displayed in a coplanar fashion, leading to the direct comparison of the two imaging modalities in terms of dimension, with a continuous updated scaling (7,15,18–20).

However, intraoperative US has limitations, particularly in the assessment of the tumor border (21–24). Contrast-enhanced US can be used to highlight neoplastic lesions and tumor vascularization, permitting the investigation of dynamic vascular phases and the analysis of tissue perfusion (15,19). Contrast material–enhanced US is an established study method for extracranial solid lesions that only recently has been applied to brain tumors (15,19,20,25–28). Our group has shown that contrast-enhanced US in GBM allows highlighting of the lesions compared with B-mode imaging, can help characterize cerebral glioma, and depicts tumor remnants during removal of GBM (15,19,20).

The aim of the current study was to use real-time fusion imaging to compare GBM contrast enhancement (location, morphologic features, margins, dimensions, and pattern) obtained with intraoperative contrast-enhanced US versus that obtained with preoperative gadolinium-enhanced T1-weighted MR imaging.

Advance in Knowledge

- In a series of 10 patients, fusion imaging of glioblastoma contrast enhancement with gadolinium-enhanced T1-weighted MR imaging and contrast-enhanced US during surgery allows for superimposed images with respect to location, margins, dimensions, and morphologic features.

Implication for Patient Care

- The information obtained with contrast-enhanced US is of potential utility in the surgical management of GBM.

Materials and Methods

Our institutional review board approved this retrospective study, and the requirement to obtain informed consent was waived.

We retrospectively evaluated intraoperative data obtained from 98 patients with histologically proved GBM who underwent surgery in the first neurosurgical division of our institution from March 2015 to December 2015. Of these patients, we included only the 10 patients in whom intraoperative fusion imaging between contrast-enhanced US and preoperative gadolinium-enhanced T1-weighted MR imaging had been performed. Fusion imaging was performed by two neurosurgeons with more than 7 years of experience in intraoperative US (F.D., F.P.). There were seven men and three women, with a mean age of 58 years (range, 49–72 years).

All lesions were supratentorial unilateral; six were left-sided and four were right-sided (Table).

Preoperative MR Imaging

Preoperative MR imaging for neuronavigation was performed 1–3 days before

Published online before print
10.1148/radiol.2017161206 **Content code:** NR

Radiology 2017; 000:1–8

Abbreviation:
GBM = glioblastoma multiforme

Author contributions:
Guarantors of integrity of entire study, F.P., V.V., M.D.B., F.D.; study concepts/study design or data acquisition or data analysis/interpretation, all authors; manuscript drafting or manuscript revision for important intellectual content, all authors; manuscript final version approval, all authors; agrees to ensure any questions related to the work are appropriately resolved, all authors; literature research, F.P., V.V., M.D.B., C.B., L.M.S., V.P., L.S., L.D., F.D.; clinical studies, F.P., V.V., M.D.B., V.P., G.M., L.D., F.D.; statistical analysis, F.P., V.V., M.D.B.; and manuscript editing, F.P., V.V., M.D.B., C.B., L.M.S., V.P., G.M., V.K., L.D., F.D.

Conflicts of interest are listed at the end of this article.

Overview of Patient Population

Patient No./Age (y)/Sex	Location at Contrast-enhanced US and MR Imaging	Margins at Contrast-enhanced US and MR Imaging	Size at MR Imaging (mm)	Tumor Size at Contrast-enhanced US (mm)	Enhancement Pattern at MR Imaging	Enhancement Pattern at Contrast-enhanced US
1/74/F	Left occipitotemporal	Defined	40 × 29	40 × 30	Nodular	Nodular
2/55/M	Right frontoparietal	Defined	42 × 32	40 × 30	Ring	Ring
3/59/M	Right frontal	Defined	25 × 28	25 × 28	Ring	Ring
4/42/F	Left frontal	Blurred	20 × 30	20 × 30	Nodular	Nodular
5/49/F	Left frontal	Defined	63 × 54	63 × 54	Ring/nodular	Ring/nodular
6/57/M	Right fronto-insular	Defined	24 × 14	24 × 14	Ring	Ring
7/62/M	Right temporal	Blurred	61 × 36	61 × 36	Ring	Ring
8/57/M	Left frontal	Defined	33 × 29	33 × 29	Ring	Ring
9/70/F	Left parietal	Blurred	43 × 31	43 × 31	Ring	Ring
10/65/M	Left temporal posterior	Blurred	35 × 23	35 × 23	Ring/nodular	Peripheral/nodular

surgery with a 1.5-T MR unit (Achieva; Philips, Amsterdam, the Netherlands). Patients underwent imaging in the supine position. The standard axial postcontrast volumetric T1-weighted sequence (fast field echo; repetition time msec/echo time msec, 7.3/3.3; matrix, 256 × 256; isotropic voxel; flip angle, 8°; section thickness, 1 mm) extended from the foramen magnum to vertex, including the nose anteriorly, and was performed after intravenous injection of contrast material (0.2 mL/kg; Magnevist; Bayer, Leverkusen, Germany).

US Examination

We used a MyLab Twice US machine (Esaote, Florence, Italy) equipped with software for fusion imaging (MedCom, Darmstadt, Germany) based on an electromagnetic tracking system (7,15,19,20). The system permits registration of the position of the US probe in the preoperative MR imaging data set, allowing the fusion of contrast-enhanced US and/or B-mode images to preoperative gadolinium-enhanced T1-weighted MR images. The probe is registered to the navigation system before each surgical procedure by using an electromagnetic tracking system by means of surface matching registration with external landmarks (7) that have previously been located in a preoperative MR imaging data set. The device shows the real-time US images (section thickness, 0.245 cm), together with the corresponding coplanar MR images, with the possibility to merge the modalities by means of superimposition (Fig E1 [online]). A 3–11-MHz linear probe (LA 332; Esaote, Napoli, Italy) at low-power mechanical index insonation was used for contrast-enhanced US (15,19,20).

For the contrast material, we used SonoVue (Bracco, Milan, Italy), which consists of sulfur hexafluoride stabilized microbubbles. Contrast-enhanced US is based on a specific algorithm (CnTI algorithm; Esaote) that analyzes the total echo signal, representing only the harmonic signal from contrast material resonance (15,19,20).

Intraoperative Contrast-enhanced US

After bone flap removal but before opening of the dura, the probe was draped in a surgical sterile transparent plastic sheath with some coupling gel and positioned over the dura. Contrast-enhanced US was preceded by standard B-mode scanning in two orthogonal planes to identify principal landmarks, the lesion, and neighboring structures and to set the US focus just below the lesion (15,18–20). Next, the insonation mechanical index was set to low power and a single 2.4-mL bolus of contrast material (5 mg/mL) was injected, followed by a 10-mL flush of saline solution for each scan. Synchronously with injection, a timer and cine clip were started to study the contrast material kinetics in the lesion from the arrival in major vessels to the washout; usually the cine clip was registered for at least 100 seconds (range, 100–300 seconds), enabling study of the lesion on both the main axis and the entire volume, along with whole vascular phases.

Comparison between Preoperative Gadolinium-enhanced T1-weighted MR Imaging and Intraoperative Contrast-enhanced US

The offline comparative analysis was based on the fusion imaging feature of the virtual navigation software, which allows display of coplanar tomographic images of intraoperative contrast-enhanced US and preoperative gadolinium-enhanced T1-weighted MR imaging; with use of the overlap function, it was possible to directly compare the two modalities.

The offline comparison between features at gadolinium-enhanced T1-weighted MR imaging and contrast-enhanced US was retrospectively performed after surgery by the neurosurgeon (F.P.), who performed the examination, and a neuroradiologist (V.V.), both of whom had more than 5 years of experience in US and contrast-enhanced US interpretation, in consensus.

For all the lesions, we qualitatively compared the contrast enhancement seen with US versus that seen with

Figure 1

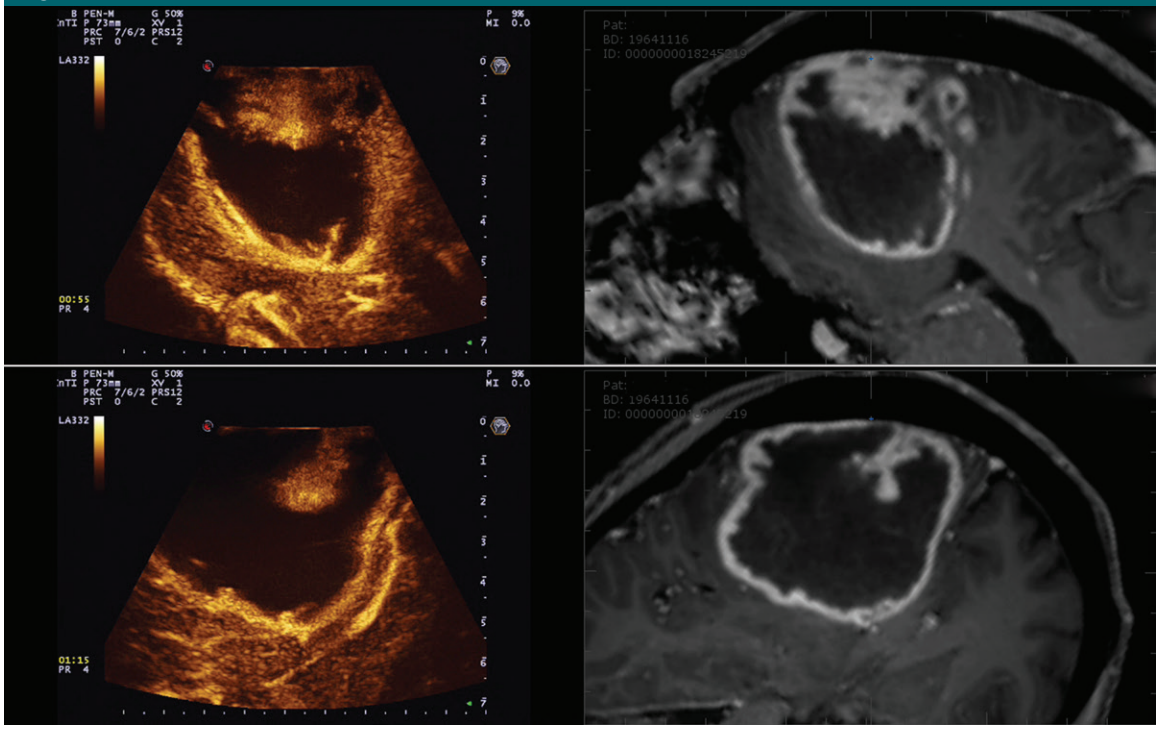

Figure 1: Navigation contrast-enhanced orthogonal US scans of left frontal GBM in 49-year-old woman. Top row, sagittal contrast-enhanced US scan (left) and corresponding coplanar preoperative MR image (right). Bottom row, coronal contrast-enhanced US scan (left) and corresponding coplanar preoperative MR image (right).

gadolinium-enhanced T1-weighted MR imaging (Figs 1, 2, E1–E3 [online]) by using the overlap function of fusion imaging. We checked for correspondence of both modalities regarding location (position of the tumor with respect to that seen with the other modality), morphologic features (shape of the tumor), margins (blurred or defined), dimensions (size on largest diameters), pattern (ring or nodular appearance), and tumor necrotic area.

In addition, we measured the largest diameters of the tumors in the axial plane at MR imaging and at contrast-enhanced US, but only for descriptive purposes.

Results

MR Imaging Evaluation

Features on postcontrast T1-weighted-weighted images were distinctive for GBM in all patients: high irregularity of tumor shapes and many concavities along the tumor outlines, regular and well-circumscribed edges, and central hypointensity encompassed by a hyperintense rim (29) (Figs 1–3 and E1–E3 [online]). The mean maximum lesion diameter was 40 mm (range, 24–63 mm) (Table).

Eight of the 10 lesions (80%) had peripheral irregular ring enhancement along the apparent borders of the mass. The margins of the ring looked wavy, and its inner aspect was shaggy and irregular. The remaining two lesions (20%) had prevalent nodular enhancement with a central necrotic component (Table).

US Analysis

B-mode US depicted the lesion in all cases (100%). Compared with normal brain tissue, all GBM lesions appeared hyperechoic and heterogeneous because of multiple well-defined nodular components and cystic and/or necrotic areas (Figs 3, E3 [online]). All lesions showed poorly defined margins.

Compared with the normal brain tissue, all GBM lesions strongly enhanced (Figs 1–3 and E1–E3 [online]), enabling clear differentiation between the surrounding brain parenchyma and the tumor. The mean maximum lesion diameter was 40 mm (range, 24–63 mm) (Table). Contrast enhancement kinetics were the same in all GBM lesions (10 of 10 lesions [100%]), demonstrating a rapid arterial wash-in and a rapid venous washout (Fig 3). In the arterial phase (2–3 seconds), chaotic transit of microbubbles within the lesion was observed, and peak enhancement was seen at 5 seconds. Transit time at contrast-enhanced US was very fast, with the venous phase at 15 seconds in all cases (Fig 3).

The major arterial supply was clearly visible, as was the venous drainage system, toward the periventricular zone (Figs E1, E2 [online]). All lesions

Figure 2

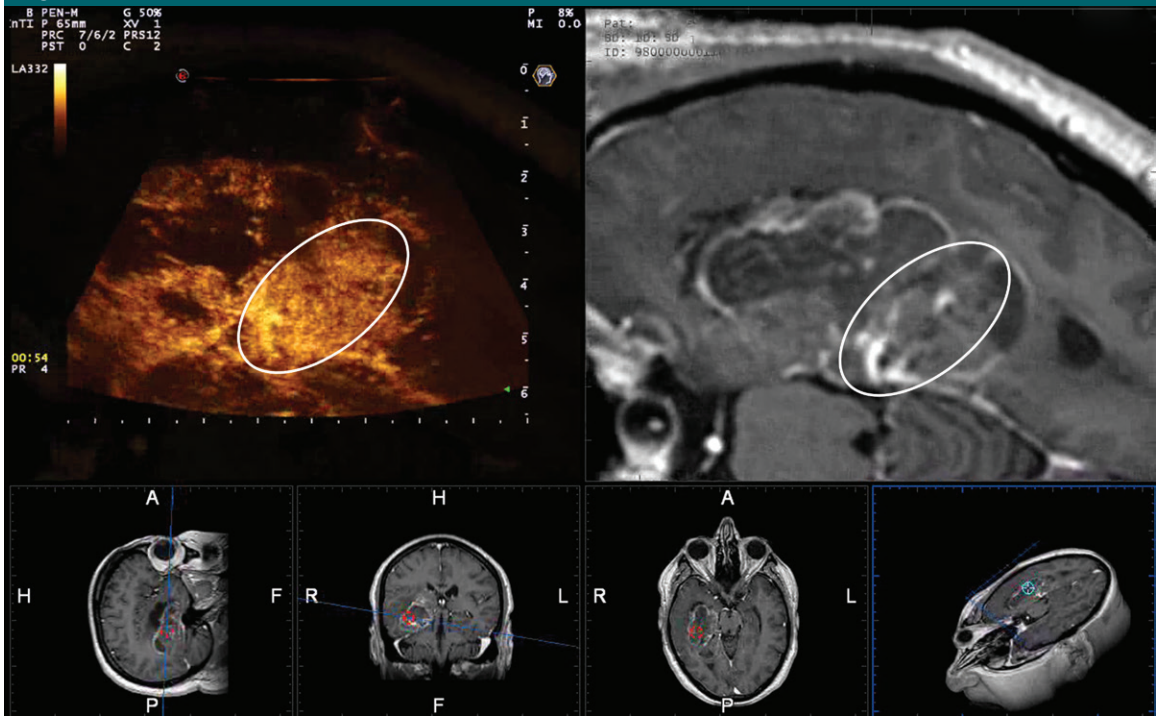

Figure 2: Screenshot of navigation contrast-enhanced US scan of left temporal GBM in 65-year-old man. Top row, contrast-enhanced US scan (left) and corresponding coplanar preoperative MR image (right). Oval indicates area with different enhancement on contrast-enhanced US scan and preoperative MR image. Bottom row, four reconstructions of preoperative MR images. Contrast-enhanced US scan demonstrates more intense contrast enhancement compared with gadolinium-enhanced T1-weighted MR image. Moreover, enhancement pattern differs. Gadolinium-enhanced T1-weighted MR imaging depicts large necrotic area surrounded by a ring-shaped solid tumor, whereas contrast-enhanced US demonstrates the part of the tumor that is extremely viable (oval). Intraoperative findings showed that this was solid tumor.

had an irregular and inhomogeneous enhancement pattern, two lesions demonstrated a nodular high-contrast dense pattern, and seven lesions demonstrated a ringlike enhancement surrounding a hypoperfused necrotic or nonperfused cystic area (Figs 1, 3, E1–E3 [online]). One lesion showed mixed internal nodular and peripheral enhancement (Fig 2). Many intratumoral vessels were observed. All lesions showed a rapid refilling (around 3–4 seconds) after rapid sonication at high mechanical index sonication.

Comparison between Preoperative Gadolinium-enhanced T1-weighted MR Imaging and Intraoperative Contrast-enhanced US

In all cases, the fusion imaging system showed images from the two imaging modalities simultaneously, with correct scaling and a positional discrepancy of less than 2 mm. The navigation system allowed a dynamic evaluation of the lesions with the US probe along different planes, with maintenance of the correspondence between images from both modalities in all cases. The location, morphologic features, margins, and dimensions of the lesions were superimposable in all cases, as shown at qualitative visual comparison by using the overlap function. The comparison of contrast-enhanced US with MR images showed the same lesion size for eight of the 10 lesions (80%), whereas for two of the 10 cases (20%), the size discrepancy was 1 and 2 mm, respectively (patients 1 and 2, Table). In particular, the margins of the lesions, evaluated on both major axes with both modalities, were similar with gadolinium-enhanced MR imaging and contrast-enhanced US, whereas tumor necrotic areas appeared larger with contrast-enhanced US.

Qualitative analysis of contrast enhancement pattern demonstrated a similar distribution in contrast-enhanced US and gadolinium-enhanced T1-weighted MR imaging in nine patients: Seven lesions showed peripheral inhomogeneous ring enhancement, and two lesions showed a prevalent nodular pattern. In one patient, the contrast enhancement pattern differed between the two modalities: Contrast-enhanced US showed enhancement of the entire bulk of the tumor, whereas gadolinium-enhanced T1-weighted MR imaging demonstrated peripheral contrast enhancement (Fig 2). In this case, the surgeon found hypervascularized GBM with massive bleeding that was unexpected on the basis of preoperative gadolinium-enhanced T1-weighted MR imaging.

Figure 3

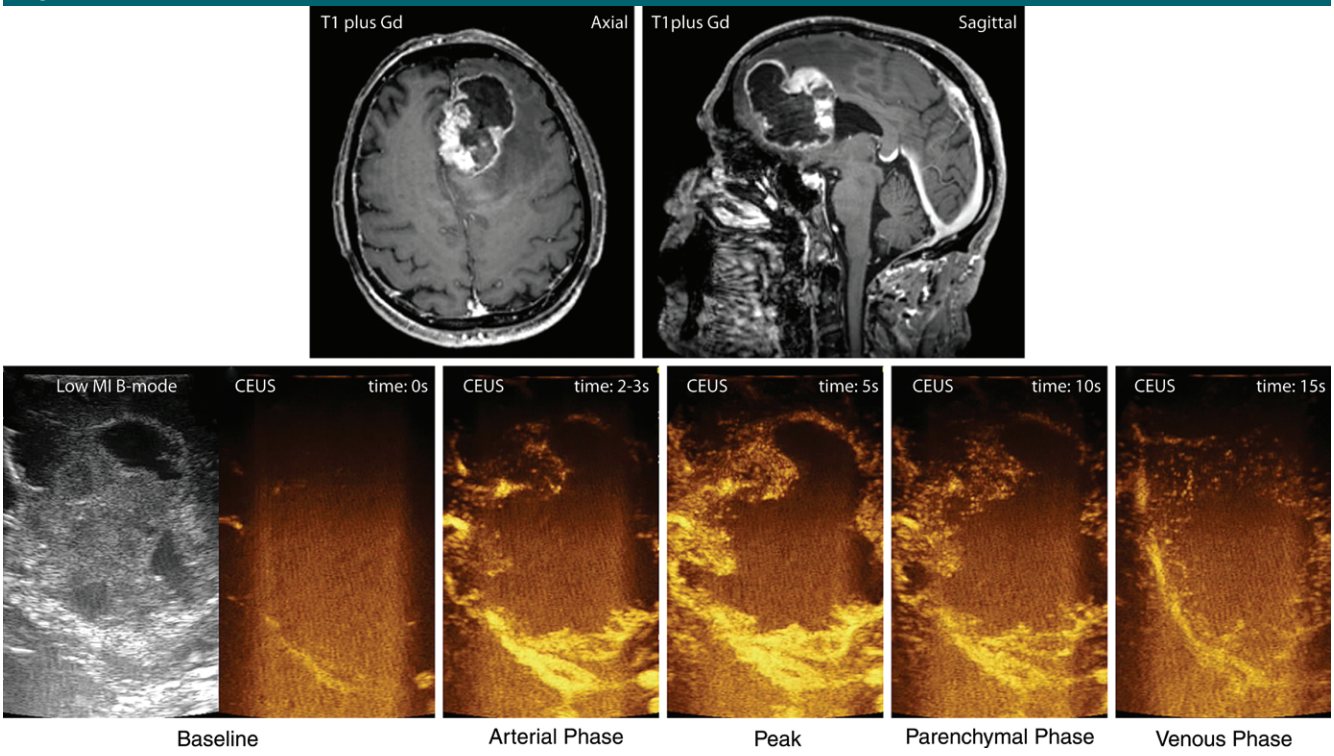

Figure 3: Contrast enhancement phases. Images of left frontal GBM in 49-year-old woman. Top row, preoperative T1-weighted gadolinium-enhanced MR images in axial and sagittal planes. Bottom row, contrast-enhanced US *(CEUS)* scans show enhancement phases. In arterial phase, main feeding arteries are visible. In peak and parenchymal phases, it is possible to distinguish more solid and cystic and/or necrotic areas. In venous phase, movement of microbubbles makes small draining veins recognizable. *Gd* = gadolinium, *MI* = mechanical index.

Discussion

Our results demonstrate that contrast-enhanced US offers a morphologic representation of GBM similar to that provided with preoperative gadolinium-enhanced T1-weighted MR imaging. The location, morphologic features, margins, and dimensions of the lesions were superimposable in all cases. The pattern of contrast enhancement was similar for both techniques in nine patients. One lesion showed more intense enhancement in the internal part of the lesion at contrast-enhanced US than at gadolinium-enhanced T1-weighted MR imaging.

Our data demonstrate that contrast-enhanced US can be used to describe the same volume target provided by preoperative gadolinium-enhanced T1-weighted MR imaging and therefore can be used as an intraoperative guidance tool. Furthermore, unlike neuronavigation, which is based on preoperative static imaging, contrast-enhanced US is dynamic, economic, and repeatable throughout surgery (15,19,20,30). Contrast-enhanced US can provide the surgeon with important information about onsite tumor location, morphologic features, margins, and dimensions for the duration of the entire surgery (15,18–20).

In our patients, the pattern of contrast enhancement was similar with both modalities in all cases but one. In that case, the tumor was highly vascularized, with profuse intraoperative bleeding from both the peripheral and central areas of the tumor. This was unexpected on the basis of preoperative gadolinium-enhanced T1-weighted MR imaging, in which contrast enhancement was prevalent peripherally, whereas contrast-enhanced US showed an intense degree of contrast enhancement of the entire bulk of the tumor, with a direct feeding vessel from the posterior choroidal artery. The different dynamic of the contrast agents at gadolinium-enhanced T1-weighted MR imaging and contrast-enhanced US may explain this phenomenon. Gadopentetate dimeglumine, after the initial vascular phase, accumulates within the lesion because of disruption of the blood-brain barrier. This is why GBM shows a prevalent peripheral enhancement that corresponds to active cell proliferation and brain tissue damage. Unlike gadopentetate dimeglumine, sulfur hexafluoride microbubbles have an intravascular distribution. Thus, the obtained image strictly reflects the vascularity of the lesion and can highlight tumoral areas with neoangiogenesis to the surrounding edematous brain tissue. It also allows the surgeon to recognize the arterial supply of the tumor and to distinguish the venous drainage (15,20,30).

This might also help explain why the internal appearance of the tumor differs

slightly with the two modalities. The internal appearance on gadolinium-enhanced T1-weighted MR images, because of contrast material extravasation within avascular and/or necrotic areas, shows a wider degree of contrast enhancement that comprises the shape of internal necrotic areas; because these areas are not perfused, they are not highlighted at contrast-enhanced US. However, this does not affect the identification of the borders and external morphologic features of the tumor and thus of the surgical target volume. The external portion of the tumor consists of biologically active areas that enhance at both modalities because it is richly vascularized by aberrant capillaries, which allow transit of microbubbles and extravasation of gadolinium.

The information provided with contrast-enhanced US in our experience was useful for appropriate surgical management of GBM. It showed perfusion patterns and tumor remnants, as our group reported elsewhere (15,18–20), but also showed a target volume superimposable to that obtained with the standard of reference, gadolinium-enhanced T1-weighted MR imaging, to identify the volume target.

The results of our study show that intraoperative contrast-enhanced US highlights in real time the amount of tumor to resect in GBM surgery because it enables visualization of the same volume target identified at preoperative gadolinium-enhanced T1-weighted MR imaging, without the limitations of neuronavigation. This is of paramount importance considering the changes that occur before and during tumor removal due to brain shift and tissue deformation; these changes affect neuronavigation systems that are based on preoperative imaging that cannot be updated (gadolinium T1-weighted MR imaging), thereby making such systems unreliable throughout surgery.

Our study has several limitations that potentially weaken our results. Inclusion bias was possible in this retrospective analysis because we included only patients in whom intraoperative fusion imaging between contrast-enhanced US and preoperative gadolinium-enhanced T1-weighted MR imaging had been performed. In addition, this fusion imaging was performed in an unblended fashion by two neurosurgeons expert in intraoperative US. The analysis was qualitative and based on the subjective evaluation of the overlap between the two imaging modalities.

Furthermore, B-mode US and contrast-enhanced US have some intrinsic limitations. For example, their application in neurosurgery is recent, and neurosurgeons lack expertise in their use. US imaging is relatively operator dependent, and the need to compare and coregister intraoperative US images with MR imaging sections is cumbersome (7). Another important limitation of intraoperative US is the lack of panoramic view, especially compared with MR imaging (7). This limitation requires the operator to accurately scan the lesion in standard B mode and to accurately analyze it after injection of the contrast agent. In addition, in certain intraoperative settings, the contrast resolution of intraoperative US is sometime slower than that of MR imaging, particularly in the differentiation between white and gray matter. Furthermore, T1-weighted gadolinium-enhanced MR imaging is actually the standard of reference for identifying the volume target to be resected. Other MR imaging sequences, such as dynamic susceptibility contrast-enhanced imaging, could be more informative with regard to tumor location or invasiveness. Indeed, dynamic susceptibility contrast-enhanced imaging depicts tissue perfusion in regions lacking damage to the blood-brain barrier, encompassing the area shown at T1-weighted gadolinium-enhanced MR imaging (31). It might be used in the future for surgical guidance that also takes into account functional boundaries. Studies comparing contrast-enhanced US with perfusion MR imaging are warranted.

In conclusion, intraoperative contrast-enhanced US during GBM surgery enables surgeons to obtain information regarding location, morphologic features, margins, and dimensions similar to that achieved with preoperative gadolinium-enhanced T1-weighted MR imaging and can be used for intraoperative guidance in removal of these tumors. Future studies should investigate the role of intraoperative US in the evaluation of residual tumor, usually a great challenge for neurosurgeons. The synergistic use of contrast-enhanced US with navigation systems and other imaging modalities, such as intraoperative MR imaging, fluorescence imaging, and optical imaging, might help maximize resection of GBM, thereby minimizing the risks for our patients.

Acknowledgments: The authors thank Caroline King, DipArch, for her kind advice in revising the manuscript and Luca Lodigiani for his technical support.

Disclosures of Conflicts of Interest: F.P. disclosed no relevant relationships. **V.V.** disclosed no relevant relationships. **M.D.B.** disclosed no relevant relationships. **C.B.** disclosed no relevant relationships. **L.M.S.** Activities related to the present article: disclosed no relevant relationships. Activities not related to the present article: received a travel grant from Bracco Imaging and Esaote. Other relationships: disclosed no relevant relationships. **V.P.** disclosed no relevant relationships. **G.M.** disclosed no relevant relationships. **L.S.** disclosed no relevant relationships. **G.S.** disclosed no relevant relationships. **V.K.** disclosed no relevant relationships. **L.D.** disclosed no relevant relationships. **M.D.** disclosed no relevant relationships.

References

1. Ostrom QT, Gittleman H, Farah P, et al. CBTRUS statistical report: primary brain and central nervous system tumors diagnosed in the United States in 2006–2010. Neuro-oncol 2013;15(Suppl 2):ii1–ii56.

2. Stupp R, Mason WP, van den Bent MJ, et al. Radiotherapy plus concomitant and adjuvant temozolomide for glioblastoma. N Engl J Med 2005;352(10):987–996.

3. Chaichana KL, Jusue-Torres I, Navarro-Ramirez R, et al. Establishing percent resection and residual volume thresholds affecting survival and recurrence for patients with newly diagnosed intracranial glioblastoma. Neuro-oncol 2014;16(1):113–122.

4. Lacroix M, Abi-Said D, Fourney DR, et al. A multivariate analysis of 416 patients with glioblastoma multiforme: prognosis, extent of resection, and survival. J Neurosurg 2001;95(2):190–198.

5. Sanai N, Polley MY, McDermott MW, Parsa AT, Berger MS. An extent of resection threshold for newly diagnosed glioblastomas. J Neurosurg 2011;115(1):3–8.

6. Dorward NL, Alberti O, Velani B, et al. Postimaging brain distortion: magnitude, correlates, and impact on neuronavigation. J Neurosurg 1998;88(4):656–662.

7. Prada F, Del Bene M, Mattei L, et al. Preoperative magnetic resonance and intraoperative ultrasound fusion imaging for real-time neuronavigation in brain tumor surgery. Ultraschall Med 2015;36(2):174–186.

8. Stieglitz LH, Fichtner J, Andres R, et al. The silent loss of neuronavigation accuracy: a systematic retrospective analysis of factors influencing the mismatch of frameless stereotactic systems in cranial neurosurgery. Neurosurgery 2013;72(5):796–807.

9. Li Y, Rey-Dios R, Roberts DW, Valdés PA, Cohen-Gadol AA. Intraoperative fluorescence-guided resection of high-grade gliomas: a comparison of the present techniques and evolution of future strategies. World Neurosurg 2014;82(1-2):175–185.

10. Barbagallo GM, Palmucci S, Visocchi M, et al. Portable intraoperative computed tomography scan in image-guided surgery for brain high-grade gliomas: analysis of technical feasibility and impact on extent of tumor resection. Oper Neurosurg (Hagerstown) 2016;12(1):19–30.

11. Kubben PL, ter Meulen KJ, Schijns OE, ter Laak-Poort MP, van Overbeeke JJ, van Santbrink H. Intraoperative MRI-guided resection of glioblastoma multiforme: a systematic review. Lancet Oncol 2011;12(11):1062–1070.

12. Moiyadi AV. Objective assessment of intraoperative ultrasound in brain tumors. Acta Neurochir (Wien) 2014;156(4):703–704.

13. Sæther CA, Torsteinsen M, Torp SH, Sundstrøm S, Unsgård G, Solheim O. Did survival improve after the implementation of intraoperative neuronavigation and 3D ultrasound in glioblastoma surgery? A retrospective analysis of 192 primary operations. J Neurol Surg A Cent Eur Neurosurg 2012;73(2):73–78.

14. Wang J, Liu X, Ba YM, et al. Effect of sonographically guided cerebral glioma surgery on survival time. J Ultrasound Med 2012;31(5):757–762 .

15. Prada F, Bene MD, Fornaro R, et al. Identification of residual tumor with intraoperative contrast-enhanced ultrasound during glioblastoma resection. Neurosurg Focus 2016;40(3):E7.

16. Hammoud MA, Ligon BL, elSouki R, Shi WM, Schomer DF, Sawaya R. Use of intraoperative ultrasound for localizing tumors and determining the extent of resection: a comparative study with magnetic resonance imaging. J Neurosurg 1996;84(5):737–741.

17. Moiyadi AV, Kannan S, Shetty P. Navigated intraoperative ultrasound for resection of gliomas: predictive value, influence on resection and survival. Neurol India 2015;63(5):727–735.

18. Prada F, Del Bene M, Casali C, et al. Intraoperative navigated angiosonography for skull base tumor surgery. World Neurosurg 2015;84(6):1699–1707.

19. Prada F, Mattei L, Del Bene M, et al. Intraoperative cerebral glioma characterization with contrast enhanced ultrasound. BioMed Res Int 2014;2014:484261 .

20. Prada F, Perin A, Martegani A, et al. Intraoperative contrast-enhanced ultrasound for brain tumor surgery. Neurosurgery 2014;74(5):542–552; discussion 552.

21. Moiyadi AV. Linear intraoperative ultrasound probes and phased-array probes: two sides of the same coin. Acta Neurochir (Wien) 2015;157(6):957–958.

22. Selbekk T, Jakola AS, Solheim O, et al. Ultrasound imaging in neurosurgery: approaches to minimize surgically induced image artefacts for improved resection control. Acta Neurochir (Wien) 2013;155(6):973–980.

23. Šteňo A, Karlík M, Mendel P, Čík M, Šteňo J. Navigated three-dimensional intraoperative ultrasound-guided awake resection of low-grade glioma partially infiltrating optic radiation. Acta Neurochir (Wien) 2012;154(7):1255–1262.

24. Šteňo A, Matejčík V, Šteňo J. Intraoperative ultrasound in low-grade glioma surgery. Clin Neurol Neurosurg 2015;135:96–99.

25. Engelhardt M, Hansen C, Eyding J, et al. Feasibility of contrast-enhanced sonography during resection of cerebral tumours: initial results of a prospective study. Ultrasound Med Biol 2007;33(4):571–575.

26. He W, Jiang XQ, Wang S, et al. Intraoperative contrast-enhanced ultrasound for brain tumors. Clin Imaging 2008;32(6):419–424.

27. Hölscher T, Ozgur B, Singel S, Wilkening WG, Mattrey RF, Sang H. Intraoperative ultrasound using phase inversion harmonic imaging: first experiences. Neurosurgery 2007;60(4 Suppl 2):382–386; discussion 386–387.

28. Kanno H, Ozawa Y, Sakata K, et al. Intraoperative power Doppler ultrasonography with a contrast-enhancing agent for intracranial tumors. J Neurosurg 2005;102(2):295–301.

29. Itakura H, Achrol AS, Mitchell LA, et al. Magnetic resonance image features identify glioblastoma phenotypic subtypes with distinct molecular pathway activities. Sci Transl Med 2015;7(303):303ra138.

30. Piscaglia F, Nolsøe C, Dietrich CF, et al. The EFSUMB Guidelines and Recommendations on the Clinical Practice of Contrast Enhanced Ultrasound (contrast-enhanced US): update 2011 on non-hepatic applications. Ultraschall Med 2012;33(1):33–59.

31. Artzi M, Blumenthal DT, Bokstein F, et al. Classification of tumor area using combined DCE and DSC MRI in patients with glioblastoma. J Neurooncol 2015;121(2):349–357.